30th Annual International IEEE EMBS Conference
Vancouver, British Columbia, Canada, August 20-24, 2008

Simulation of skin reflectance images using 3D tissue modeling and multispectral Monte Carlo light propagation

Vincent C. Paquit, Fabrice Mériaudeau, *Member, IEEE*,
Jeffery R. Price, *Member, IEEE* and Kenneth W. Tobin., *Senior Member, IEEE*

***Abstract*— In this work we propose a method to simulate the expected, i.e. seen by a camera, multispectral reflectance images of a large skin surface area by combining Monte Carlo light propagation model and realistic tissue modeling based on three dimensional data acquisition of human body areas. In particular, we aim to simulate more accurately light transport in biological tissue by taking into account the geometrical topography of the skin surface, the structure and optical properties of the skin layers, and the subcutaneous veins in presence. We describe our computation method in detail and present simulated reflectance images results.**

***Index Terms*— Monte Carlo simulation, 3D modeling, structured light ranging, Near-Infrared venous imaging**

I. Introduction

Previous studies have investigated statistical models to simulate light propagation phenomena in the skin by considering the molecular and structural nature of the tissues and their optical properties. With theses methods, one can simulate the energy distribution in the tissues including the diffuse reflectance characteristics that will match experimental measurements for small skin surface areas. However, current methods do not consider the three dimensional nature of the scene, i.e. curvature of the surface and shape of the blood vessels, and then cannot be applied to simulate diffuse reflectance images of large skin surface areas including subcutaneous structures. In this paper, we propose a method to simulate realistic reflectance imagery of the skin, including veins, by combining 3D modeling, ray tracing and Monte Carlo light propagation modeling. The paper is organized as follows. Section II presents an overview of the current state of the art, we detail our methodology in Section III, and then we present some preliminary results in Section IV. Section V concludes the paper.

II. State of the Art

Biomedical imaging techniques based on wave propagation phenomena in biological tissues are commonly used to detect and treat diseases but are also used to image non-invasively organs and biological structures inside the body. Amongst them, optical tomography is a growing imaging technique offering the advantages to be non-invasive, experimentally simple, repeatable and inexpensive. Optical tomography uses light which offers at specific wavelengths a large variety of interaction phenomena, functions of physiological changes at cellular and subcellular levels, and allows retrieving information on biological systems. Over the last decade, publications in the field have reported promising results [1] as well as really surprising images [2] of human or animal organs, letting us envision the capabilities of biomedical imaging using light. However, in this field only few researches investigate subcutaneous veins visualization and measurement.

Using light propagation properties of tissues in the near infrared range of light, Zeman et al. [3] developed and commercialized, via Luminetx, a device to locate subcutaneous veins and back project their position on the imaged skin surface for catheter insertion assistance. The device named VeinViewer works well on the average person, but performance can be decreased significantly based on poorly understood relations to various physiological parameters. This technology also provides no estimation of the relative depth or diameter of vessels, which are key factors in selecting the optimal vein. Nishidate et al. [4] introduced a method aiming to locate and measure subcutaneous veins by analyzing diffuse reflectance images of a large skin area at different wavelengths. Their experimental results on tissue phantom are in accordance with the theory computed with Monte Carlo models. However, their results on real tissues imaging present significant errors that we believe are due to non-consideration of the 3D topography of the surface and subsurface structures.

In computer graphics, skin rendering is probably one of the current most challenging researches. In general, most methods compute reflectance images by combining 3D modeling of the scene and different light propagation models. Donner et al. [5] present probably the best results so far. In this field, the objective is to give the illusion of a realistic rendering of the skin color excluding, for computation time minimization, all nearly invisible subcutaneous structures. Then, these models cannot be applied directly to our research and have to be modified to include subcutaneous veins.

III. Methodology

A. Light propagation methods

Light propagation in biological tissues is well described in classic mechanics and quantum mechanics, respectively defining the dynamic of the oscillating electromagnetic field and the energy transfers with the medium. Both approaches being difficult to implement in the case of highly scattering turbid medium, one usually chose to simulate light

Manuscript received April 16, 2008.

V.C. Paquit and F. Mériaudeau are with the Le2i Laboratory, University of Burgundy, Le Creusot, France (e-mail: paquitvc@ornl.gov)

J.R. Price and K.W. Tobin, Jr are with the Oak Ridge National Laboratory, Oak Ridge, TN 37831 USA

propagation using Monte Carlo modeling [6] or Kubelka-Munk theory [7], where light propagation is characterized by five basic optical events: reflection, refraction, diffusion, absorption and transmission. These phenomena depend on several interaction parameters (anisotropy factor, refractive index, absorption coefficient and scattering coefficient) and are described by mathematical equations reported in [8]. In this work we use a Monte Carlo based method [9] to compute the diffuse reflectance values since it has been proven to give more accurate simulation results than Kubelka-Munk models, when compared with experimental measurements on living tissues.

B. Skin structure and optical properties

Anatomically, the skin is divided into three principal layers: epidermis, dermis and hypodermis; subdivision based on the physiological functions they assume and their molecular structure. In [10], Meglinski et al. present a seven layer model in order to improve existing Monte Carlo methods. The optical parameters difference amongst layers being not always significant, we have opted for a three layer model listed thereafter (from top to bottom):

- the Epidermis contains a large fraction of the chromophores of the skin defining the overall skin tone;
- the Dermis contains blood vessels or nerves, and structural molecules;
- the Hypodermis is the lowest layer of the skin, also called subcutaneous tissue. Composed of fat and connective tissues, it contains large blood vessels.

We have listed Table I the skin layers optical parameters used in the simulation presented in this paper for two separate wavelengths, data compiled from literature [11]:

TABLE I
SKIN OPTICAL PARAMETERS USED IN THE MONTE CARLO SIMULATIONS

			500nm		700nm		
	n	g	$\mu_s(\lambda)$	$\mu_a(\lambda)$	$\mu_s(\lambda)$	$\mu_a(\lambda)$	d
Epidermis	1.34	0.765	219.29	11.87	108.07	3.88	0.01
Dermis	1.40	0.765	219.29	1.94	108.07	0.21	0.20
Hypodermis	1.44	0.750	15.35	1.06	12.21	1.36	0.05
Blood vein	0.98	0.980	474.75	121.11	308.23	1.55	0.52
Hypodermis	1.44	0.750	15.35	1.06	12.21	1.36	1.00

The absorption $\mu_a(\lambda)$ and scattering $\mu_s(\lambda)$ coefficients are given in cm^{-1}, refractive index n and anisotropy factor g are dimensionless. The thickness d is given in cm.

C. Skin surface modeling

The majority of the Monte Carlo models simplify the propagation medium to a system with infinitely parallel layers [6], [10]. In this configuration, photons enter in the medium orthogonally to the surface, leading to a uniform specular reflection on the entire surface, and the passage from one layer to another is just based on depth verification and not on structural particularities. In order to correct this problem, we integrate three dimensional capabilities to our model using parametric surfaces as layer transitions. We compute the 3D shape of the skin model based on real skin tissue images, captured using active optical triangulation for range data acquisition. With this method we aim to compute the directional cosines of the photon entering the skin and accurately simulate the interaction propagation of the photon in the medium with curved transition interfaces such as blood vessel walls.

D. Experimental setup

Our acquisition system is composed of a visible to NIR sensitive CMOS video camera, a NIR line-generating laser module and a broadband illumination source (Hg arc lamp) associated with a monochromator for illumination wavelength selection. The equipment is controlled by a computer to synchronize illumination selection and image capture. In order to avoid UV radiation injuries to the skin, a high-pass filter at 495nm is inserted between the lamp and the monochromator. The spectral range of study is comprised between 495nm and 945nm, and can be incremented by step of 1nm, the upper limit being determined by the spectral sensitivity of the camera in the near infrared. A liquid gel light guide is connected on one hand to the output of the illumination source and on the other hand to a two inches wide collimating probe to obtain uniform illumination on the surface of the skin. The line generating laser module is used to retrieve the shape of the skin surface using active optical triangulation. Figure 1 is a schematic of the acquisition system. The calibration of the system consists in three separate steps: (1) image distortion correction by retrieving the optical parameters of the camera [12], (2) reflectance image computation using black and white spectralons as references [13], (3) parameterization of the triangulation geometry [14].

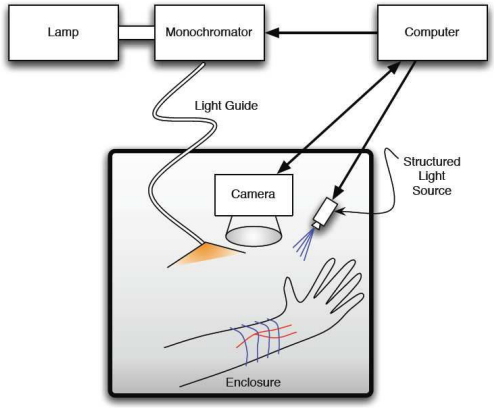

Fig. 1. Schematic of the acquisition system

1) 3D reconstruction: Our 3D reconstruction process of the skin surface combines active optical triangulation for range data acquisition, and parametric surface modeling to store the 3D shape of the object. Active optical triangulation [14] combines a camera and a laser stripe line generator to create a basic geometric system as shown Figure 2. The camera is aligned along the Z axis and the laser line generator is positioned at a distance b from the camera with the angle θ relative to the X axis. Assuming that the considered laser point coordinates (x, y, z) in the 3D baseline has a projection

(u,v) on the image plane, the similar triangles equations give the mathematical relation between the measured quantities (u,v,θ) and the coordinates (x,y,z):

$$[x,y,z] = \frac{b}{f.\cot\theta - u}[u,v,f]. \quad (1)$$

Parameters b, f and θ are calculated during the system calibration and remain constant during the acquisition phase. In a NIR image of the laser lines on the surface of the

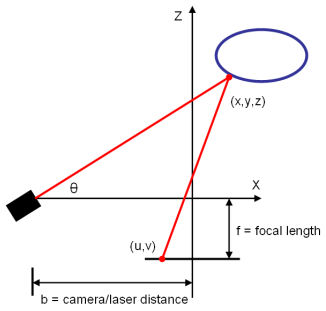

Fig. 2. Optical triangulation principle

skin, Figure 3, the centerline of each line is detected using a curvilinear structures detector and then triangulated using Equation 1, see Figure 3.

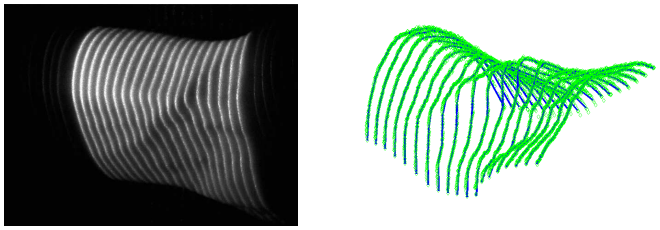

Fig. 3. (left) NIR image of the laser lines, (right) approximation of the 3D Point cloud (green) with Bézier curves (blue)

2) Bézier surface: To simplify the three-dimensional surface modeling of the skin, we approximate the triangulated point cloud with a Bézier surface, concept introduced by Pierre Bézier in 1972 to design automobile bodies with a simplified modeling method [15]. We parameterize the 3D surface of the skin with a $(m \times n)$ dimensional Bézier patch defined by a set of $(m+1) \times (n+1)$ control points $C_{i,j}$. Each point P on the surface being approximated over the unit square as a function of two parametric coordinates u and v by the following equation:

$$P(u,v) = \sum_{i=0}^{m} B_i^m(u) \left[\sum_{j=0}^{n} B_j^n(v)\, C_{i,j} \right] \quad (2)$$

with $B_i^m(u)$ and $B_j^n(v)$ Bernstein polynomials.Equation 2 is in fact a tensor product and can be written as a product of invertible matrices as follow:

$$\mathbf{P}(u,v) = \mathbf{M}_{B_i^m(u)} \times \mathbf{M}_{C_{i,j}} \times \mathbf{M}^T_{B_j^n(v)} \quad (3)$$

In this case, $\mathbf{P}(u,v)$ is the matrix of the triangulated points, and $\mathbf{M}_{B_i^m(u)}$ and $\mathbf{M}_{B_j^n(v)}$ are Bernstein polynomial matrices. The matrix $\mathbf{M}_{C_{i,j}}$ corresponding to the Bézier control points is then calculated from (3):

$$\mathbf{M}_{C_{i,j}} = \mathbf{M}^{-1}_{B_i^m(u)} \times \mathbf{P}(u,v) \times (\mathbf{M}^T_{B_j^n(v)})^{-1} \quad (4)$$

The dimensions m and n of the control point matrix are evaluated by fitting error minimization with a precision value ε arbitrary defined.

3) Bézier clipping: Bézier clipping is a ray tracing method used to computed the intersection between a Bézier patch and a ray [16]. By identifying and cutting away regions of the patch that are not intersecting the ray, the algorithm converge by dichotomy to a list of all acceptable intersection points for a given initial precision value ε, including the 3D coordinates of the points and the coordinates of the normal to the surface. In our simulation we consider the illumination direction to be collinear to the Z axis. As a result, the angle of incidence for each point of the surface can be calculated as the scalar product between the normal to the surface and the direction vector of the light beam. Using this method, we can compute for each pixel of the region of interest, the elevation map and the incident angles map to the surface.

IV. Results

Using our acquisition system, we capture three images of a skin surface area where we can visually see a blood vessel: a visible range image at 500nm, a NIR image at 700nm, and an image with the structured light pattern. We then reconstruct the 3D model of the skin according to the methods detailed in Paragraph III-C and assuming each sublayer as a homothety of the surface layer in order to maintain equal space between them. In the NIR image, where the contrast vein/skin is higher, we locate the central path of a blood vessel in the (XY) plane using a curvilinear detector [17] and estimate its average width. The center path is parameterized with a Bézier curve. Assuming we are visualizing a near surface vein, we consider that the blood vessel follow the curvature of the skin, and modify the central path parameterization accordingly. Figure 4 gives a representation of the skin model used in our simulation.

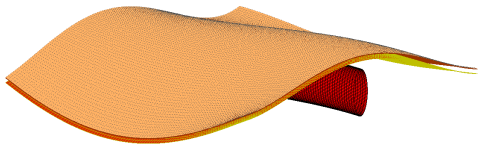

Fig. 4. 3D model of the skin surface: layer transitions are represented with large surfaces and a blood vessel is positioned in the hypodermis. Layers and vessel are parameterized with Bézier patches

Using the Bézier clipping algorithm we compute the elevation map and the normal to the surface for each pixel of the final reflectance image. The normal coordinates are then converted into incident angles. Figure 5 presents the computation results of the elevation map in order to appreciate the 2D topography of the skin and the incident angles map used for the specular reflection evaluation.

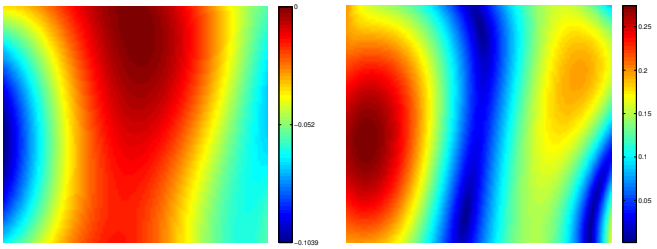

Fig. 5. Geometric parameters computed on the 3D model Figure 4 using Bézier Clipping: (left) elevation map of the surface of the skin (unit: inch), (right) angle variations between the normal to the surface and the incident light direction (unit: rad)

Then we compute the diffuse reflectance values for each pixel. Notice that in a cylindrical referential as used in [8], the diffuse reflectance can be computed using our parameters with approximately 5000 photons. However, there is no central symmetry with our approach, so we have to simulate the diffuse reflectance in two dimensions instead of one to obtain stable reflectance values, requiring around 200,000 photons in total for the same simulation. This difference increases significantly the processing time of our method compare to [8]. Figures 6 and 7 present the simulation results of the reflectance images of the scene at 500nm and 700nm. One can see in the colormap images the expected reflectance variations due to the skin surface topography and that the subcutaneous vein is almost invisible at 500nm when the contrast at 700nm is important, as noticed in the reflectance images captured.

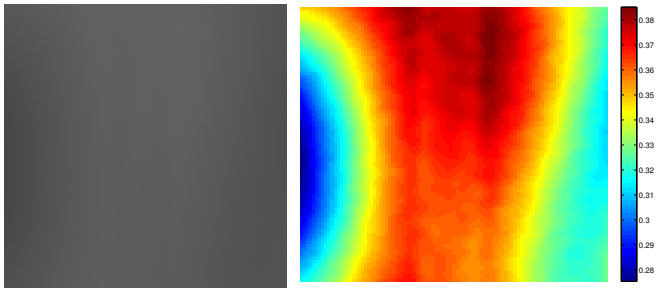

Fig. 6. Reflectance image of the skin at 500nm: (left) reflectance image simulated, (right) colormap image of the reflectance values to enhance the intensity variations visualization. The colorbar indicates the reflectance range.

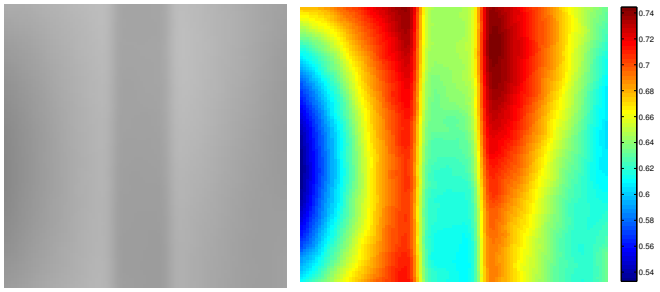

Fig. 7. Reflectance image of the skin at 700nm: (left) reflectance image simulated, (right) colormap image of the reflectance values to enhance the intensity variations. The colorbar indicates the reflectance range.

V. Conclusion and Future Work

In this paper we present a method to simulate theoretical reflectance images of the human skin under a variety of illuminants by combining realistic 3D Monte Carlo light propagation, and 3D modeling of the skin surface and the subcutaneous structures. We are currently investigating performance evaluation between our method and a modified MCML version [8] in order to quantify the computational complexity versus the performance gained. In addition we are currently evaluating the accuracy of our method by comparing simulation results with captured reflectance images of tissue phantoms with known optical and structural characteristics.

References

[1] Elizabeth M. C. Hillman, *Experimental and theoretical investigations of near infrared tomographic imaging methods and clinical applications*, Ph.D. thesis, University of London, London, UK, 2002.

[2] Elizabeth M. Hillman and Anna Moore, "All-optical anatomical co-registration for molecular imaging of small animals using dynamic contrast," *Nat Photon*, vol. 1, no. 9, pp. 526–530, 2007.

[3] Herbert D. Zeman, Gunnar Lovhoiden, Carlos Vrancken, and Robert K. Danish, "Prototype vein contrast enhancer," *Optical Engineering*, vol. 44, no. 8, pp. 086401, 2005.

[4] I. Nishidate, T. Maeda, Y. Aizu, and K. Niizeki, "Visualizing depth and thickness of a local blood region in skin tissue using diffuse reflectance images.," *J Biomed Opt*, vol. 12, no. 5, pp. 054006, 2007.

[5] Craig Donner and Henrik Wann Jensen, "A spectral shading model for human skin," in *SIGGRAPH '06: ACM SIGGRAPH 2006 Sketches*, New York, NY, USA, 2006, p. 147, ACM.

[6] S. A. Prahl, M. Keijzer, S. L. Jacques, and A. J. Welch, "A Monte Carlo model of light propagation in tissue," in *SPIE Proceedings of Dosimetry of Laser Radiation in Medicine and Biology*, 1989, vol. IS 5, pp. 102–111.

[7] Paul Kubelka, "New contributions to the optics of intensely light-scattering materials. part i," *J. Opt. Soc. Am.*, vol. 38, no. 5, pp. 448–457, 1948.

[8] W. Lihong, S.L. Jacques, and Z. Liqiong, "MCML - monte carlo modeling of light transport in multi-layered tissues," *Computer Methods and Programs in Biomedicine*, vol. 47, pp. 131–146(16), July 1995.

[9] Vincent Paquit, Jeffery R. Price, Fabrice Meriaudeau, and Kenneth W. Tobin, "3d multispectral light propagation model for subcutaneous veins imaging," 2008, vol. 6913, p. 69130D, SPIE.

[10] Igor V Meglinski and Stephen J Matcher, "Quantitative assessment of skin layers absorption and skin reflectance spectra simulation in the visible and near-infrared spectral regions," *Physiological Measurement*, vol. 23, no. 4, pp. 741–753, 2002.

[11] S. L. Jacques, "Skin optics," 1998, http://omlc.ogi.edu/news/jan98/skinoptics.html.

[12] Janne Heikkila and Olli Silven, "A Four-step Camera Calibration Procedure with Implicit Image Correction," in *CVPR '97: Proceedings of the 1997 Conference on Computer Vision and Pattern Recognition (CVPR '97)*, Washington, DC, USA, 1997, p. 1106, IEEE Computer Society.

[13] Zhihong Pan, Glenn Healey, Manish Prasad, and Bruce Tromberg, "Face recognition in hyperspectral images," *IEEE Transactions on Pattern Analysis and Machine Intelligence*, vol. 25, no. 12, pp. 1552–1560, 2003.

[14] Paul J. Besl, *Surfaces in range image understanding*, Springer-Verlag New York, Inc., New York, NY, USA, 1988.

[15] Pierre E. Bezier, *Emploi des machines a commande numerique*, Masson et Cie., 1970, Translated by Forrest, A. Robin and Pankhurst, Anne F. as Numerical Control – Mathematics and Applications, John Wiley and Sons, Ltd., London, 1972.

[16] Alexander Efremov, Vlastimil Havran, and Hans-Peter Seidel, "Robust and numerically stable bezier clipping method for ray tracing nurbs surfaces," in *SCCG 2005*. 2005, pp. 123–131, ACM.

[17] C. Steger, "Extraction of curved lines from images," in *13th International Conference on Pattern Recognition*, 1996, vol. 2, pp. 251–255.